Development 126, 1859-1868 (1999)
Printed in Great Britain © The Company of Biologists Limited 1999
DEV8586

Novel guidance cues during neuronal pathfinding in the early scaffold of axon tracts in the rostral brain

R. B. Anderson and B. Key*

Neurodevelopment Laboratory, Department of Anatomy and Cell Biology, University of Melbourne, Parkville 3052, Australia
*Author for correspondence (e-mail: bkey@anatomy.unimelb.edu.au)

Accepted 16 February; published on WWW 6 April 1999

SUMMARY

A scaffold of axons consisting of a pair of longitudinal tracts and several commissures is established during early development of the vertebrate brain. We report here that NOC-2, a cell surface carbohydrate, is selectively expressed by a subpopulation of growing axons in this scaffold in *Xenopus*. NOC-2 is present on two glycoproteins, one of which is a novel glycoform of the neural cell adhesion molecule N-CAM. When the function of NOC-2 was perturbed using either soluble carbohydrates or anti-NOC-2 antibodies, axons expressing NOC-2 exhibited aberrant growth at specific points in their pathway. NOC-2 is the first-identified axon guidance molecule essential for development of the axon scaffold in the embryonic vertebrate brain.

Key words: Carbohydrate, Axon guidance, Cell surface molecule, Tract, Development, Growth cone

INTRODUCTION

The trajectory of major axon tracts in the vertebrate brain is established early in development by pioneer axons, which grow along defined pathways (Wilson and Easter, 1991; Ross et al., 1992). The guidance cues used by growing axons during formation of this scaffolding are largely unknown. There is some evidence that axons navigate along the boundaries of expression domains of regulatory genes within the anterior neuroepithelium (Wilson et al., 1993; Macdonald et al., 1994, 1997). However, the target genes within these regulatory cascades are unknown. Once pioneer axons are established, they serve as a template for later growing axons to follow (Kuwada, 1986; Chitnis and Kuwada, 1991). The labelled pathways hypothesis proposed that molecules present on the surface of pioneer axons are used as guidance cues for the growth cones of later growing axons (Raper et al., 1983). Numerous attempts have been made to identify cell surface molecules that exhibit restricted expression patterns in neural tissue, particularly on cells and axons within pathways followed by growing axons. This approach led to the identification of several cell adhesion molecules as axon guidance cues in invertebrates (Harrelson and Goodman, 1988; Snow et al., 1988; Elkins et al., 1990; Grenningloh et al., 1990; Lin et al., 1994). In contrast, most vertebrate cell adhesion molecules, such as N-CAM and L1, are widely expressed within the embryonic vertebrate brain. NOC-1 is one of only a few cell surface molecules described to date that have a restricted distribution in the early scaffold of axon tracts in vertebrates (Anderson and Key, 1996).

Much of our understanding of axon guidance in the vertebrate brain comes from studies of the retinal pathway. However these axons enter the brain relatively late in development, only after the initial scaffold of axon tracts has been established. Nonetheless, these studies have provided valuable information about the principles of axon guidance in vertebrate brain. Retinal axons use a combination of guidance cues as they navigate from the eye, along the optic stalk, through the optic chiasm, to the optic tract and finally the optic tectum. For instance, retinal axons utilise local positional cues, present within the neuroepithelium underlying the optic tract, to orient towards their target. When small regions of neuroepithelium underlying the presumptive optic tract were rotated, retinal axons entering the rotated tissue were deflected in the direction of the rotation (Harris, 1989). Examination of mutants in zebrafish have demonstrated that sequential cues demarcate a continuous pathway for retinal axons from the eye to the tectum (Baier et al., 1996; Karlstrom et al., 1996). This pathway consists of a number of major choice or decision points that axons navigate en route to their target.

Apart from studies of the retinal pathway there is little understanding of how specific subpopulations of axons are selectively guided at critical choice points within the early scaffold of axon tracts in vertebrate brain. What are the cues that direct growing axons to join, grow along and exit specific axon tracts within the early scaffold? Some candidate guidance molecules were uncovered when it was revealed that discrete forebrain axon tracts in the adult frog brain selectively expressed novel cell surface glycoconjugates (Key and Akeson, 1990, 1991). One of these molecules, NOC-1, was expressed by a distinct subpopulation of axons within the embryonic *Xenopus* forebrain (Anderson and Key, 1996). NOC-1^+ axons followed a stereotypical pathway and appeared to sort out and selectively fasciculate within some axon tracts. We postulated that these as well as other cell surface carbohydrates provide a chemical code used for axon recognition and guidance in the

embryonic brain. In the present study we describe the presence of a novel cell surface carbohydrate NOC-2 that is expressed by a discrete subpopulation of axons in *Xenopus*. Furthermore, we demonstrated a role for NOC-2 in axon guidance in situ using an exposed brain preparation.

MATERIALS AND METHODS

Animals

Embryos were obtained from the induced mating of adult *Xenopus laevis borealis* frogs by injection of human chorionic gonadotropin hormone (Sigma Chemical Company, St Louis, MO). Embryos were reared in 10% Holtfreter's solution (Holtfreter, 1943) at 20°C and staged according to Nieuwkoop and Faber (1956). For immunohistochemistry embryos were fixed in 4% paraformaldehyde in 0.1 M Tris-buffered saline (TBS) (0.9% NaCl in 0.1 M Tris, pH 7.4) for 12 hours.

Whole-mount immunohistochemistry

A histochemical screen on whole mounts of embryonic *Xenopus* brain was undertaken using a panel of plant lectins and anti-carbohydrate antibodies (Table 1). The mouse anti-acetylated α-tubulin monoclonal antibody was obtained commercially from ICN Biochemicals Inc. (Costa Mesa, CA, USA) and was used to label all axons within the *Xenopus* brain (Chu and Klymkowsky, 1989; Hartenstein, 1993). Monoclonal antibodies against the human blood group A (BGA) trisaccharide were purchased from the Commonwealth Serum Laboratories (IgM; Melbourne, Australia) and Accurate Chemicals, (IgG; NY, USA). The 162 rabbit polyclonal anti-N-CAM antiserum recognises the three major isoforms of N-CAM (Akeson et al., 1988).

Whole brains of stage 32 *Xenopus* embryos were dissected and dehydrated in a graded ethanol series (70% to 100%). Embryos were washed in ethanol:propylene oxide (1:1) for 5 minutes, followed by 10- and 20-minute washes in 100% propylene oxide. After washing in ethanol:propylene oxide (1:1) for a further 5 minutes, brains were rehydrated through a graded ethanol series (100% to 70%) to TBS. The brains were then incubated for 1 hour in 2% (w/v) bovine serum albumin (BSA) and 0.3% (v/v) Triton X-100 (TX-100) (Sigma Chemical Co.) before reacting with various lectins and monoclonal antibodies (see Table 1). Following a brief wash in TBS, embryos were reacted with primary antibodies followed by an appropriately labelled secondary antibody and then visualised using either Extravidin-FITC or -TRITC (60 μg/ml) (Sigma). Embryos reacted with biotinylated lectins (20-50 μg/ml) were diluted in 2% BSA and 0.3% TX-100 containing 1 mM of $MgCl_2$, $MnCl_2$ and $CaCl_2$, washed and then incubated with Extravidin-TRITC (60 μg/ml).

For double-label immunofluorescence, embryos were first incubated with the acetylated α-tubulin antibody and processed as described above using Extravidin-FITC. Embryos were then incubated with the anti-BGA antibody followed by a TRITC-conjugated goat anti-mouse IgM secondary antibody (1:50) (Jackson Immunoresearch Laboratories Inc., West Grove, PA). Control embryos that were reacted with either one of the primary antibodies and with both secondary antibodies revealed no cross-reactivity of reagents. Some embryos were also double-labelled using anti-NOC-1 antibodies (IgM; Anderson and Key, 1996) and anti-BGA antibodies (IgG; Accurate Chemicals).

Whole mounts of *Xenopus* brains were viewed using either an Olympus BH2-RFC microscope fitted with epifluorescence optics or an MRC-1024 Biorad laser-scanning confocal microscope coupled to a Zeiss Axioplan microscope. Images were digitized on a Kodak RFS-1200 scanner, colour-balanced using Photoshop 4.0 (Abode Systems Incorporated, CA) and assembled with Coreldraw 7.0 (Corel Corporation Limited, Dublin, Ireland).

Immunoblotting and immunoprecipitation

The brains of *Xenopus* embryos were dissected and homogenized in TBS containing 2 mM EDTA and a cocktail of protein inhibitors (0.1 mM phenylmethanesulfonyl fluoride, 500 units/ml Kallilrein inhibitor, 1 μg/ml aprotinin and 1 μg/ml pepstatin A) to obtain a crude membrane preparation as previously described (Key and Akeson, 1990). Protein content was determined by the Lowry method using BSA as standard. Membranes were boiled for 5 minutes in Laemmli's sample buffer and electrophoresed on a 6% discontinuous SDS-polyacrylamide gel. Proteins were subsequently electrotransferred to Hybond-ECL nitrocellulose (Amersham International, UK) in 25 mM Tris-glycine buffer (pH 8.3) containing 0.1% SDS and 20% methanol. Blots were blocked in 100 mM Tris (pH 7.4) containing 0.9% NaCl, 0.3% TX-100 and 5% BSA and then reacted with the appropriate antibodies and visualized using enhanced chemiluminescence (Amersham International). Controls that were reacted with non-specific antibodies and treated as above revealed no labelled bands.

N-CAM was immunoprecipitated from the brain membrane preparation as previously described (Key and Akeson, 1991). Briefly, Omnisorb cells (Calbiochem, CA) were treated for 15 minutes in a solubilization buffer containing 2% BSA and 0.3% TX-100 in TBS and then coated with the anti-N-CAM antiserum (20 μl/50 μl of Omnisorb cells) for 2 hours. Following two brief washes by centrifugation, the Omnisorb-antibody complex was resuspended and incubated with the membrane extract (50 μl of Omnisorb cells/500 μg of membrane protein) for 1 hour. The membrane extract was presorbed with Omnisorb cells alone for 15 minutes. The Omnisorb-antibody-antigen complex was washed three times by centrifugation before boiling in Laemmli's sample buffer for 5 minutes.

Since the mouse anti-BGA monoclonal antibody (Commonwealth Serum Laboratories) was an IgM, which binds very poorly to Omnisorb cells, an antibody sandwich technique was used to immunoprecipitate NOC-2. Omnisorb cells were first coated with an affinity-purified goat anti-mouse IgM antibody (Sigma) (10 μg/10 μl of Omnisorb cells) for 1 hour before reacting with the anti-BGA antibody (10 μg/10 μl of Omnisorb cells) for a further 2 hours. This complex was subsequently reacted with the brain membrane preparation (10 μl of Omnisorb cells/150 μg of membrane protein) for 2 hours. All immunoprecipitations were repeated at least five times and yielded consistent results.

Xenopus whole-mount cultures

Stage-26 *Xenopus* embryos were anaesthetized with tricaine methanesulfate (0.4 mg/ml) and cultured in modified Barth's solution (100 mM NaCl, 2 mM KCl, 2 mM $CaCl_2$, 1 mM $MgCl_2$, 5 mM Hepes and 50 μg/ml gentamicin) containing 0.1% dimethyl sulfoxide as previously described (Chien et al., 1993; Anderson et al., 1998). The ectoderm overlaying the left side of the embryo was removed using glass micropipettes to expose the underlying brain. The TPOC was ablated by lesioning with a glass micropipette the nucleus of the TPOC, which lies ventral to the eye. Unsuccessful or incomplete ablations were treated as sham controls. The following reagents were added to the culture media: lactose (1, 2 and 10 mM) (Sigma); synthetic BGA trisaccharide (1 and 2 mM) (Accurate Chemicals, NY); BGA-human serum albumin conjugate (1 and 4 μM) (Accurate Chemicals); human serum albumin (1 and 4 μM) (Accurate Chemicals); purified anti-BGA antibody (50 μg/ml) (Commonwealth Serum Laboratories) and purified mouse IgM (50 μg/ml) (Sigma). The BGA-human serum albumin neoglycoprotein contained 19 moles of trisaccharide per mole of albumin. Embryos were maintained at 27°C for up to 12 hours, before being fixed in 4% paraformaldehyde and analysed by whole-mount immunohistochemistry.

RESULTS

A subpopulation of forebrain axons express novel glycoconjugates

At stage 32 (approx. 40 hours post-fertilisation) the embryonic

Xenopus brain consists of a simple scaffold of axon tracts, as revealed by immunostaining for acetylated α-tubulin (Fig. 1A). A schematic diagram of axon pathways is presented in Fig. 1B. The embryonic *Xenopus* forebrain has a principal longitudinal axon tract, the tract of the postoptic commissure (TPOC) that is present bilaterally. This tract courses along the ventrolateral surface of the forebrain and merges with the ventral longitudinal tract in the midbrain. There is one prominent ventral

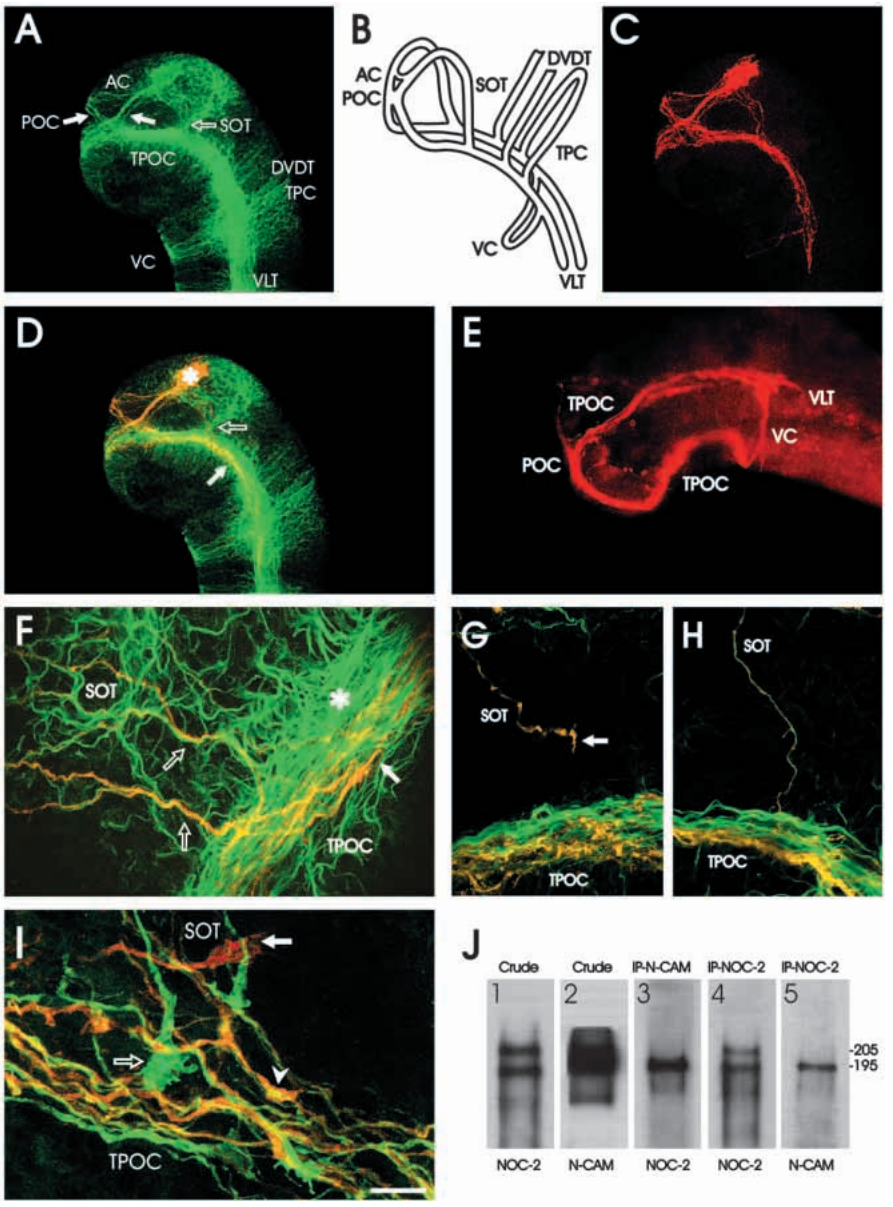

Fig. 1. Immunostaining of subpopulations of axons in the embryonic *Xenopus* brain. (A) Confocal image of a whole-mount *Xenopus* brain at stage 32 immunostained for acetylated α-tubulin to reveal all growing axons. The brain is viewed from the ventrolateral surface; dorsal is to the top and rostral to the left. The principal longitudinal tract of the forebrain is the tract of the postoptic commissure (TPOC) that merges with the ventral longitudinal tract (VLT) of the midbrain. The ventral commissure (VC) crosses the ventral midline and connects axons in the TPOC on either side of the brain. The rostral surface of the forebrain contains the anterior commissure (AC) and the postoptic commissure (filled arrows, POC). Axons arising from the nucleus of the presumptive telencephalon (nPT) give rise to the supraoptic tract (unfilled arrow, SOT) that courses ventrally to merge with the TPOC. Two ventrally directed axon tracts also merge with the TPOC: the dorsoventral diencephalic tract (DVDT) and the tract of the posterior commissure (TPC). (B) Schematic diagram of the bilateral symmetry of the early scaffold of axon tracts in the *Xenopus* embryonic brain. (C) Double-label of the same embryo as in A with anti-blood group A trisaccharide antibodies. NOC-2 expressing axons are stained in red. (D) Merged image of A and C reveals that NOC-2 is expressed by a subpopulation of axons coursing in the SOT (unfilled arrow), TPOC (filled arrow) as well as the anterior, postoptic and ventral commissures. A small number of axons have entered the rostral portion of the ventral longitudinal tract in this embryo. Asterisk, presumptive telencephalon. (E) Reflected light immunofluoresence image of a stage-32 *Xenopus* brain stained for NOC-2. This embryo is viewed from the ventral surface, which reveals the circular trajectory of NOC-2^+ axons around the rostral brain. Axons project along the TPOCs on both sides of the brain and cross the midline via the POC and ventral commissure (VC). Some axons continue growing caudally and project from the TPOC into the ventral longitudinal tract (VLT), which is only visible on one side in this orientation. (F) High magnification confocal image of the junction between the SOT and TPOC labelled for NOC-2 (red) and acetylated α-tubulin (green). Caudal is to the upper right side of the panel. Double-stained axons appear yellow. NOC-2^+ axons course preferentially in the ventral region of the TPOC (filled arrow) rather than in the dorsal aspect of this tract (asterisk). NOC-2^+ axons in the SOT (unfilled arrrows) merge with NOC-2^+ axons in the ventral region of the TPOC. (G-H) Confocal images of the pioneer axon in the SOT double labelled for NOC-2 (red) and acetylated α-tubulin (green). (G) The pioneer axon and its growth cone (arrow) expresses NOC-2 and acetylated α-tubulin as it grows ventrally toward the TPOC. (H) The pioneer axon in the SOT fasciculates with NOC-2^+ axons in the ventral region of the TPOC. (I) Confocal image of the junction of the SOT and TPOC double-labelled for NOC-1 (red) (Anderson and Key, 1996) and NOC-2 (green). Three distinct subpopulations of axons and growth cones were observed: axons expressing NOC-1 alone (filled arrow); axons expressing NOC-2 alone (unfilled arrow); and axons co-expressing both NOC-1 and NOC-2 (arrowhead). (J) Characterization of NOC-2 glycoproteins in embryonic *Xenopus* brain. Lanes 1 and 2, immunoblots of crude brain membranes stained for NOC-2 and N-CAM. NOC-2 runs as two bands at 195 and 205 kDa. N-CAM is present as a broad smeared band centered at 200 kDa. Lane 3, N-CAM was immunoprecipitated (IP) and stained for NOC-2. NOC-2 is present as a single 195 kDa glycoform of N-CAM. Lane 4, NOC-2 was immunoprecipitated and stained for NOC-2. NOC-2 was present as two bands at 195 and 205 kDa, as in crude extracts in lane 1. Lane 5, NOC-2 was immunoprecipitated and stained for N-CAM. NOC-2 was present on a single N-CAM glycoform at 195 kDa, as in lane 3. Bar, 100 μm (A,C-E), 50 μm (F), 25 μm (G,H), 20 μm (I).

commissure that connects the TPOCs on either side of the brain at the level of the ventral flexure. The rostral surface of the forebrain contains two commissures: the post-optic commissure (POC) and the anterior commissure. Axons arising from the nucleus of the presumptive telencephalon cross either to the contralateral TPOC via the POC or to the contralateral telencephalon via the anterior commissure. The TPOC therefore forms a continuous loop of axons around the ventral forebrain through the post-optic and ventral commissures. There are three small tracts linking dorsal structures to the TPOC. The supra-optic tract (SOT) originates in the presumptive telencephalon and courses around the optic vesicle to merge with the TPOC. Both the dorsoventral diencephalic tract and the tract of the posterior commissure contain axons which project ventrally and fasciculate with the TPOC.

We undertook a histochemical screen of whole mounts of stage 32 *Xenopus* brains using a panel of plant lectins and anti-carbohydrate antibodies with the aim of identifying cell surface carbohydrates differentially expressed on subpopulations of axons (Table 1). Most of these reagents either failed to react with *Xenopus* tissue or produced a ubiquitous staining pattern. However, a monoclonal antibody that recognizes the human blood group A trisaccharide, selectively labelled axon tracts within the embryonic *Xenopus* brain (Fig. 1C). The endogenous carbohydrate identified by this monoclonal antibody was referred to here as NOC-2 (for novel carbohydrate-two).

Embryos double-labelled for acetylated α-tubulin and NOC-2 revealed that NOC-2 was expressed by only a subpopulation of axons in the developing axon scaffold (Fig. 1D). NOC-2 was present on axons coursing within the SOT, TPOC and ventral longitudinal tract as well as by axons crossing within the anterior, postoptic and ventral commissures. Axons in the tract of the posterior commissure and the dorsoventral diencephalic tract did not express NOC-2. Axons expressing NOC-2 (NOC-

Table 1. The results of histochemical screening of whole mounts of *Xenopus* embryonic brain using a panel of plant lectins and anti-carbohydrate antibodies

Antibody/lectin	Epitope/ligand	Staining
[1]Murine mAb* anti-blood group A	GalNAcα1-3-Gal1β-R | Fucα1-2	Axon specific
[1]Murine mAb anti-blood group B	Galα1-3-Galβ1-R | Fucα1-2	Global
[1]Murine mAb anti-blood group H	Galβ1-3-GlcNAc-R | Fucα1-2	Absent
[1]Murine mAb anti-blood group M	Sialic acid-αGal \ R / Sialic acid-αGal	Absent
[1]Murine mAb anti-blood group N	Sialic acid-αGal \ R / αGal	Absent
[2]Human anti-blood group Pi	Galα1-4Galβ1-4GlcNAcβ1-3Gal1-4Glc	Global
[1]Murine mAb anti-blood group Le^a	Galβ1-3GlcNAcβ1-R | Fucα1-4	Global
[1]Murine mAb anti-blood group Le^b	Galβ1-3GlcNAcβ1-R | | Fucα1-2 Fucα1-4	Global
[1]Murine mAb anti-blood group Le^x	Galβ1-4GlcNAcβ1-R | Fucα1-3	Absent
[3]Murine mAb 5A5	Polysialic acid	Global
[4]*Dolichos biflorus* agglutinin	α-D-GalNAc	Global
[4]*Ulex europaeus* agglutinin	α-L-Fuc	Global
[4]*Agaricus bisporus* agglutinin	D-Gal1β-3-D-GalNAc	Global
[4]*Erythrina corallodendron* agglutinin	D-Gal1β-4-D-GlcNAc	Global
[4]*Erythrina cristagalli* agglutinin	D-Gal1β-4-D-GlcNAc	Global
[4]*Bauhinia purpurea* agglutinin	D-Gal1β-3-D-GalNAc	Global

*mAb, monoclonal antibody; [1]Commonwealth Serum Laboratories, [2]Gamma Biologicals Inc., Houston, TX, [3]Dodd and Jessell (1988), [4]Sigma Chemical Company.

Table 2. Percentage of embryos displaying aberrant trajectories of NOC-2$^+$ axons at the junction of the supraoptic tract and the tract of the postoptic commissure (SOT-TPOC), within the postoptic commissure (POC), and at the TPOC-ventral commissure junction (TPOC-VC)

	% of embryos		
Reagent	SOT-TPOC	POC	TPOC-VC
1 mM BGA	82 (17)	92 (24)	72 (18)
2 mM BGA	83 (18)	96 (26)	73 (26)
1 μM BGA-HSA	67 (12)	82 (11)	80 (10)
4 μM BGA-HSA	78 (9)	88 (8)	80 (10)
50 μg/ml anti-BGA	71 (7)	75 (4)	86 (14)
Control	0 (33)	0 (33)	0 (33)

Number of embryos, *n*, in parentheses.

2$^+$) arose from labelled neurons in the nucleus of the presumptive telencephalon (Fig. 1D, asterisk) and either crossed the midline in the anterior and postoptic commissures or grew ventrally within the SOT (Fig. 1D, unfilled arrow). Axons in the anterior commissure cross the midline to the contralateral nucleus of the presumptive telencephalon while axons in the POC enter the contralateral TPOC. Interestingly, NOC-2$^+$ axons in the TPOC course selectively within bundles in the ventral region of this tract (Fig. 1D, filled arrow) and either cross the midline again in the ventral commissure of the rostral midbrain or continue growing caudally within the ventral longitudinal tract. NOC-2$^+$ axons form a loop around the rostroventral brain, which is clearly depicted in ventral views of labelled embryos (Fig. 1E). Axons coursed longitudinally within the TPOCs and were connected across the midline via the postoptic and ventral commissures (Fig. 1E). A subpopulation of ventrally growing axons within the SOT expresses NOC-2 (Fig. 1F, unfilled arrows). These axons merge with the TPOC and appear to selectively fasciculate with axons expressing NOC-2 in the ventral region of this tract (Fig. 1F, filled arrow). In doing so the NOC-2$^+$ axons in the SOT course over axons in the dorsal half of the TPOC that do not express NOC-2 (Fig. 1F, asterisk). NOC-2$^+$ axons in the SOT never continued growing ventrally past the TPOC. Instead, all NOC-2$^+$ axons in the SOT turned at the SOT-TPOC junction and grew within the ventral TPOC. These results suggested to us that NOC-2 was involved in recognition and selective fasciculation at this choice point in the trajectory of SOT axons. If NOC-2 was involved in axon guidance it should be expressed by the first axons that navigate along the SOT towards the TPOC. Therefore we examined embryos at stage 28 when the first axons are growing within the SOT. Double-labelling of the SOT at this stage revealed that the first SOT axon and its growth cone expressed NOC-2 (Fig. 1G, arrow). Moreover, this axon grew over the dorsal TPOC and only fasciculated with axons in the ventral region of this tract (Fig. 1H). Thus, the expression pattern of NOC-2 is consistent, both spatially and temporally, with this molecule playing a role in axon guidance at the SOT-TPOC junction.

We previously identified a novel cell surface carbohydrate called NOC-1 (Key and Akeson, 1990; Anderson and Key, 1996), which is expressed on a subpopulation of axons that follow a similar pathway to that of NOC-2$^+$ axons. In order to determine whether NOC-1 and NOC-2 were expressed on the same axons in the early scaffold of axon tracts in *Xenopus* we double-labelled embryos with antibodies against these carbohydrates (Fig. 1I). Immunostaining revealed three distinct subpopulations of axons at the SOT-TPOC junction: axons that expressed NOC-1 alone (Fig. 1I, filled arrow); axons that expressed NOC-2 alone (Fig. 1I, unfilled arrow); and axons that expressed both NOC-1 and NOC-2 (Fig. 1I, arrowhead). Therefore the early scaffold of axon tracts contains several chemically distinct subpopulations delineated by expression of different cell surface carbohydrates.

NOC-2 is present on a glycoform of N-CAM

To begin to characterise the NOC-2 containing glycoproteins, crude membrane fractions of embryonic *Xenopus* brains were separated by SDS-gel electrophoresis, western blotted and reacted with the NOC-2 antibody. Two distinct bands were obtained at 195 and 205 kDa (Fig. 1J, lane 1), which resembled the previously reported banding pattern for NOC-1 present on N-CAM in frog brain (Key and Akeson, 1990). When adjacent lanes of whole brain were stained with rabbit anti-N-CAM antiserum, bands were localised at 140 kDa and across a broad smear encompassing the 195 and 205 kDa bands (Fig. 1J, lane 2). To determine whether NOC-2 was present on N-CAM we immunoprecipitated N-CAM and cross-reacted it with the NOC-2 antibody. N-CAM immunoprecipitated from brain ran as two distinct bands: a broad band centered at 200 kDa and a weaker 140 kDa band as in crude membranes in lane 2 (Fig. 1J). Immunoblotting with the NOC-2 antibody revealed that NOC-2 was expressed on a single 195 kDa glycoform of N-CAM (Fig. 1J, lane 3). These results were then confirmed by immunoprecipitating NOC-2 containing glycoproteins from brain using the NOC-2 antibody. Immunoprecipitated NOC-2 was present as two distinct bands at 195 and 205 kDa (Fig. 1J, lane 4) as previously demonstrated in the crude membrane blots in lane 1 (Fig. 1J). Only the single 195 kDa band was detected when immunoprecipitated NOC-2 was cross-reacted with N-CAM (Fig. 1J, lane 5). These results demonstrated that NOC-2 was present on both a novel 195 kDa glycoform of N-CAM as well as on an as yet unidentified glycoprotein at 205 kDa.

NOC-2-mediated turning at a specific choice point

In order to assess the role of NOC-2 in the growth and guidance of axons we used an exposed brain preparation that maintains an in vivo-like development of axon tracts (Anderson et al., 1998). The surface ectoderm and mesenchyme covering the left side of the head of stage-26 *Xenopus* embryos were prosected to expose the forebrain and embryos were then cultured in a defined medium for up to 12 hours. We postulated that selective interactions between NOC-2$^+$ axons were mediating turning of SOT axons at the SOT-TPOC junction. We initially addressed the role of these interactions by physically lesioning the TPOC before the ventrally growing SOT axons had reached the longitudinal tract (Fig. 2A). The ventral growth of NOC-2$^+$ axons in the SOT was then assessed in the absence of the TPOC by fixing animals at stage 32 and staining them with NOC-2 antibodies. In all embryos in which the TPOC had been effectively ablated (n=12), aberrant growth of NOC-2$^+$ axons in the SOT was consistently observed at the SOT-TPOC junction (Fig. 2C). Interestingly, while some NOC-2$^+$ axons continued to grow along their ventral trajectory (Fig. 2C, unfilled arrow) other axons managed to turn appropriately in the absence of the TPOC (Fig. 2C, filled arrow). The relative number of axons that

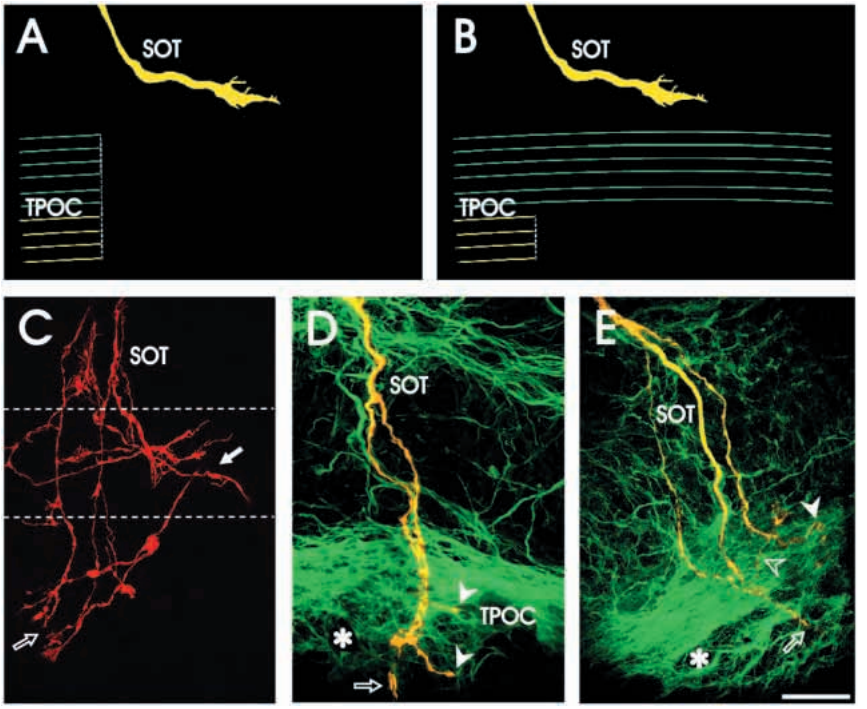

Fig. 2. Lesions of the TPOC disrupt axon growth at the SOT-TPOC junction. (A,B) Schematic drawings of lesion experiments. (A) Axons in the TPOC were lesioned before NOC-2$^+$ axons in the SOT had reached the junction of the two tracts. NOC-2$^+$ axons navigated this choice point in the absence of any TPOC axons. (B) Axons in the ventral region of the TPOC were ablated. In these embryos, no NOC-2$^+$ axons were observed in the ventral TPOC. (C) In the absence of any TPOC axons, NOC-2$^+$ axons in the SOT either continued growing ventrally (unfilled arrow) or turned appropriately (dotted lines) and grew caudally (arrow). (D-E) Confocal images of the SOT-TPOC junction double-labelled for NOC-2 (red) and acetylated α-tubulin (green) following ablation of the ventral TPOC. Double-labelled axons appear yellow. No NOC-2$^+$ axons were observed in the ventral TPOC (asterisk). (D) Axons in the SOT either continued growing ventrally past the TPOC (unfilled arrow) or turned correctly within the TPOC (filled arrowheads). (E) Three distinct axon trajectories were observed at the SOT-TPOC junction following ablation of the ventral TPOC. Axons in the SOT either continued growing ventrally (unfilled arrow), meandered in the TPOC (filled arrowhead), or turned and grew dorsally (unfilled arrowhead). Bar, 25 μm (C-E).

grew aberrantly at the SOT-TPOC junction was not determined since SOT axons course in small bundles that repeatedly defasciculate and refasiculate along their trajectory, making it difficult to assess their numbers reliably in whole-mount brain preparations. Nevertheless, qualitative assessments clearly revealed that aberrant growth occurred at the SOT-TPOC junction in all embryos with a lesioned TPOC. In contrast, in control embryos (n=15) all NOC-2$^+$ axons in the SOT turned at the SOT-TPOC junction and projected along the TPOC. SOT axons never grew ventrally past the TPOC in these embryos,

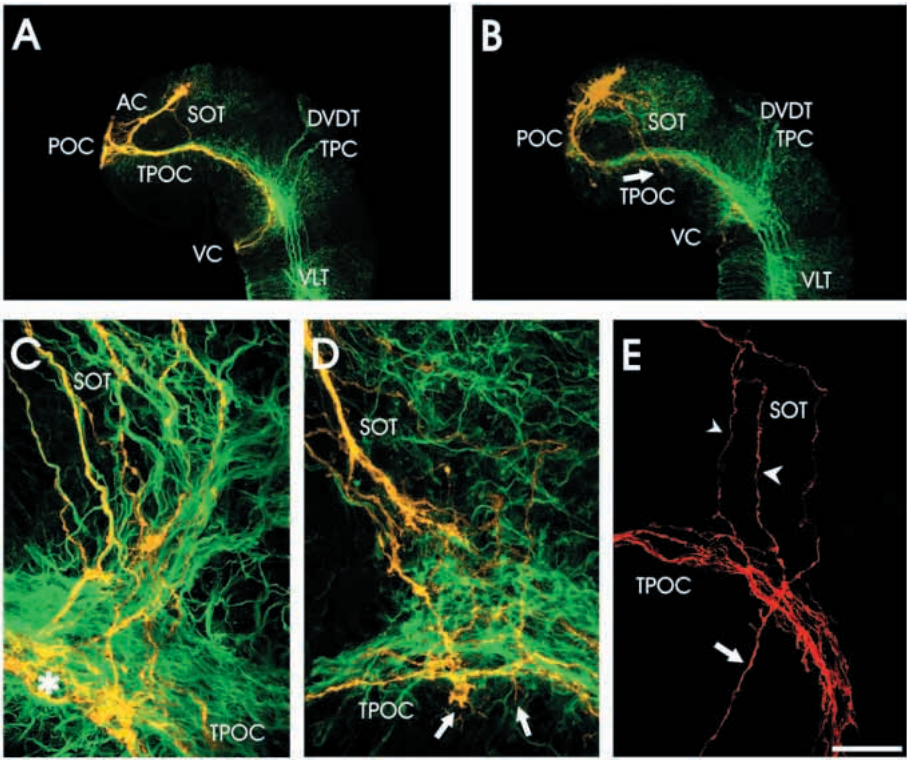

Fig. 3. Confocal microscope images of exposed brain preparations cultured in the presence of exogenous blood group A (BGA) trisaccharides. (A) Whole mount of control brain cultured in 4 mM lactose. The brain was stained for NOC-2 (red) and acetylated α-tubulin (green). The development of axon tracts is normal. (B) Brain exposed to 1 mM BGA and stained for NOC-2 (red) and acetylated α-tubulin (green). The overall development of axon tracts (green) is normal. However, there are specific defects in the trajectory of NOC-2$^+$ axons. In particular, an axon in the SOT continues to grow ventrally at the SOT-TPOC junction (arrow). Aberrant growth is also observed in the POC and in the VC. (C) High magnification of the SOT-TPOC junction in a control brain exposed to 4 mM lactose. No NOC-2$^+$ axons in the SOT extend ventrally past the TPOC (asterisk). (D) Control brain exposed to 1mM BGA displays aberrant growth at the SOT-TPOC junction. Growth cones of SOT axons grow over NOC-2$^+$ axons in the TPOC and enter inappropriate ventral territories (arrows). (E) Brain exposed to 1mM BGA-HSA displays aberrant growth at the SOT-TPOC junction. Two NOC-2$^+$ axons (arrowheads) in the SOT turn correctly at the SOT-TPOC junction while another axon continues its ventral growth and overshoots the TPOC (arrow). POC, postoptic commissure; AC, anterior commissure; SOT, supraoptic tract; TPOC tract of the POC; DVDT, dorsoventral diencephalic tract; TPC, tract of the posterior commissure; VC, ventral commissure; VLT, ventral longitudinal tract. Bar, 100 μm (A,B), 25 μm (C-E).

which indicated that the SOT-TPOC junction was an important choice point in the guidance of ventrally growing NOC-2$^+$ axons. Although some of the ventrally growing NOC-2$^+$ axons in the SOT are dependent on cues in the TPOC for correct turning, other cues at this junction also appear to be important in guiding SOT axons following lesions of the TPOC.

Next we examined the role of axons in the ventral region of the TPOC in mediating turning of NOC-2$^+$ axons in the SOT at the SOT-TPOC junction. When the ventral-most region of the TPOC was selectively ablated, NOC-2$^+$ axons were absent from the TPOC. Thus, we examined the growth of NOC-2$^+$ axons in the SOT as they projected towards the TPOC devoid of axons expressing NOC-2, but which still contained other axons (Fig. 2B). Acetylated α-tubulin immunostaining confirmed the presence of the dorsal TPOC following ablation of the ventral axons (Fig. 2D-E). The effectiveness of the ventral ablation in eliminating NOC-2$^+$ axons was demonstrated by immunostaining with the NOC-2 antibody. Ventral ablations were performed on 30 embryos; however, in six cases the ablations were unsuccessful in the total elimination of all NOC-2$^+$ axons within the TPOC and these animals were treated as sham controls. In both unablated control embryos (n=35) and sham controls (n=6), NOC-2$^+$ axons in the SOT were always observed to turn and project normally along NOC-2$^+$ axons within the ventral region of the TPOC. Aberrant trajectories occurred in all embryos with complete ablations of NOC-2$^+$ axons in the TPOC (n=24; Fig. 2D,E, asterisk). In these animals, NOC-2$^+$ axons in the SOT exhibited several different aberrant trajectories at the SOT-TPOC junction. NOC-2$^+$ axons either turned appropriately in the TPOC (Fig. 2D,E, arrowheads) or they continued growing ventrally past the TPOC (Fig. 2D,E, unfilled arrows). Those axons that turned within the TPOC subsequently displayed aberrant growth and either coursed dorsally (Fig. 2E, unfilled arrowhead) or meandered within the TPOC (Fig. 2E, filled arrowhead) rather than growing longitudinally as in control embryos. These results suggested that interactions between NOC-2$^+$ axons within the SOT and ventral region of the TPOC were important for the turning and longitudinal growth of NOC-2$^+$ axons at the SOT-TPOC junction. However, because some NOC-2$^+$ axons in the SOT turned normally there are probably additional turning cues other than those present on NOC-2$^+$ axons in the TPOC.

Although the lesion experiments revealed that the SOT-TPOC junction was an important choice point for ventrally growing SOT axons, the molecular mechanism underlying the cellular interactions at this junction remained unresolved. One possibility was that NOC-2 acted as a ligand for a carbohydrate-binding receptor or lectin present at the SOT-TPOC junction. To test this idea we cultured exposed *Xenopus* brain preparations in the presence of either exogenous soluble human blood group A (BGA) trisaccharides (1 and 2 mM) or neoglycoproteins consisting of BGA conjugated to human serum albumin (BGA-HSA) (1 and 4 μM) in order to competitively inhibit the putative receptor. We used neoglycoproteins, since previous reports indicated that sugars presented on a protein backbone are better ligands for lectins than soluble sugars. The binding affinity for free sugars to some lectins is in the 1 mM range, whereas neoglycoproteins yield binding affinities around 1 μM (Nelson et al., 1995). We observed no difference in the resultant phenotypes in the presence of either free sugars or neoglycoproteins at any of the concentrations used (Table 2).

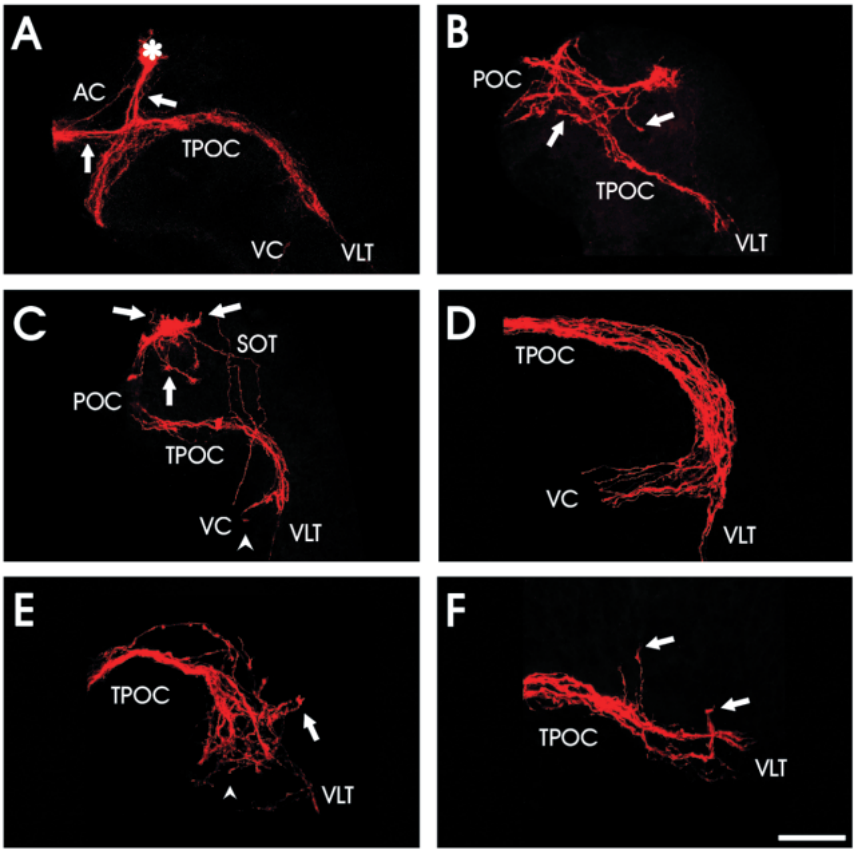

Fig. 4. Confocal microscope images of exposed brain preparations cultured in the presence of exogenous BGA trisaccharides. (A) Rostroventral surface of control brain preparation exposed to 4 mM lactose and stained for NOC-2. Axons arising in the nucleus of the presumptive telencephalon (asterisk) cross the midline in tightly fasciculated bundles in the POC (arrows). After crossing the midline these axons course caudally within the TPOC and either cross the midline again via the VC or continue into the VLT. (B) Exposed brain cultured in the presence of 2 mM BGA reveals that NOC-2$^+$ axons in the POC are defasciculated and project into inappropriate forebrain regions (arrows). Axon growth in the TPOC appears unaffected. (C) Lateral view of a brain exposed to 1 μM BGA-HSA. Aberrant growth of NOC-2$^+$ axons is observed as axons (arrows) exit inappropriately from the nucleus of the presumptive telencephalon. NOC-2$^+$ axons turnabout in the ventral commissure (arrowhead). (D) Higher magnification of the TPOC-VC junction in a control brain exposed to 4 mM lactose. NOC-2$^+$ axons in the TPOC either turn and cross the midline in the VC or continue growing caudally in the VLT. (E,F) NOC-2$^+$ axons in the TPOC display aberrant growth at the TPOC-VC junction in the presence of 2 mM BGA. Axons either form whorls (arrowhead) or turn and grow dorsally (arrows) rather than cross the midline via the VC. POC, postoptic commissure; AC, anterior commissure; SOT, supraoptic tract; TPOC tract of the POC; VC, ventral commissure; VLT, ventral longitudinal tract. Bar, 100 μm (A-C), 25 μm (D-F).

Control cultures were incubated in the presence of either the dissacharide lactose (n=10; 1, 2 and 10 mM), or HSA (n=8; 1 and 4 μM), or in unsupplemented medium (n=15). As previously reported (Anderson et al., 1998), these embryonic brains developed normally even in the presence of high concentrations of lactose (10 mM). There were no aberrant axon projections when assessed by immunostaining for acetylated α-tubulin and NOC-2 (Fig. 3A). NOC-2^+ axons within the SOT coursed ventrally toward the TPOC where they turned and grew along NOC-2^+ axons within the ventral region of this tract (asterisk, Fig. 3C), as they do in vivo. The overall formation of the early scaffold of axon tracts was also normal in brains exposed to exogenous BGA carbohydrates and BGA-HSA (Fig. 3B). Immunostaining for acetylated α-tubulin revealed that all the major tracts formed in these embryos (Fig. 3B). However, highly selective defects were observed in the trajectory of NOC-2^+ axons. In particular, NOC-2^+ axons in the SOT overshot the TPOC and continued to grow ventrally in 67-83% of embryos (Fig. 3B,D,E, arrows; Table 2). Interestingly, embryos always contained some NOC-2^+ axons in the SOT that were unaffected by exogenous BGA or BGA-HSA and turned normally at the SOT-TPOC junction (Fig. 3E, arrowheads) as previously demonstrated in the TPOC lesion experiments. NOC-2^+ axons never grew ventrally past the TPOC in control embryos (asterisk, Fig. 3C).

In addition to defects in the trajectory of NOC-2^+ axons at the SOT-TPOC junction, embryos cultured in the presence of BGA or BGA-HSA also displayed aberrant growth of NOC-2^+ axons within the POC and the ventral commissure. In control embryos (n=33), NOC-2^+ axons in the POC grew in tight bundles across the midline (Fig. 4A, arrows) whereas in 82-96% of treated animals these axons defasciculated within the POC and grew aberrantly into inappropriate forebrain regions (Fig. 4B,C, arrows; Table 2). NOC-2^+ axons either exit the TPOC and cross the ventral midline via the ventral commissure or continue growing caudally into the ventral longitudinal tract in control animals (Fig. 4D). However, in the presence of exogenous BGA, NOC-2^+ axons in the TPOC exhibited abnormal trajectories at their junction with the ventral commissure. NOC-2^+ axons failed to cross within the ventral commissure and formed whorls at the TPOC-ventral commissure junction in 72-80% of embryos (Fig. 4C,E, arrowheads; Table 2). Some axons also looped back and grew dorsally into the midbrain (Fig. 4E,F, arrows). Interestingly, despite aberrant growth within the SOT, POC and ventral commissure, the longitudinal growth of NOC-2^+ axons within the ventral region of the TPOC was unaffected by exogenous BGA carbohydrates (Fig. 4B,C).

Blocking of endogenous NOC-2 disrupts axon tract formation

The results of the above experiments supported a role for NOC-2 in the guidance of axons at the SOT-TPOC and TPOC-ventral commissure junctions as well as along the POC in the early scaffold of axon tracts in embryonic *Xenopus* brain. However, the effects mediated by exogenous carbohydrates do not necessarily imply a direct functional role for endogenous NOC-2 since BGA may be interacting with receptors that are not normally exposed to NOC-2 in vivo. Therefore we addressed this possibility by exposing brain preparations to purified anti-BGA antibody (50 μg/ml) in order to directly block endogenous NOC-2. Control cultures were incubated in either purified mouse IgM (50 μg/ml) or in unsupplemented medium. The ability of anti-BGA antibodies to penetrate brain preparations and specifically bind to NOC-2^+ axons was demonstrated by staining cultured brains exposed to these antibodies directly with fluorescein-labelled secondary antibodies. The resultant staining pattern was identical to that observed in our immunohistochemical analysis of fixed normal brains, indicating that antibodies freely diffuse into the live whole brain preparations. Embryonic brains cultured in the presence of either purified mouse IgM (n=12) or unsupplemented medium (n=12) developed normally with no aberrant axon projections, as revealed by immunostaining for acetylated α-tubulin. The trajectory of NOC-2^+ axons within these cultured brains was also normal. As in controls, the gross topography of the early scaffold of axon tracts was normal in brains exposed to anti-BGA antibodies. However, NOC-2^+ axons displayed highly selective axon guidance defects in 71-86% of treated embryos. These disruptions were similar to those previously described in embryos cultured in the presence of exogenous BGA trisaccharides and BGA-containing neoglycoproteins. For example, NOC-2^+ axons within the SOT bypassed the TPOC and continued along their ventral trajectory in 71% of embryos (Table 2). Defective phenotypes were also observed within the POC (75%) and ventral commissure (86%). NOC-2^+ axons within the POC defasciculated and were observed growing into inappropriate forebrain regions, while NOC-2^+ axons within the ventral commissure failed to cross the midline and formed whorls at the TPOC-ventral commissure junction (Table 2). In summary, these results provide compelling support for a role of endogenous NOC-2 in mediating important recognition events during navigation of NOC-2^+ axons within the embryonic vertebrate brain.

DISCUSSION

In order for a cell surface molecule to be recognized as an axon guidance cue it must satisfy a number of criteria. First, it must be present either within or surrounding the pathway followed by an axon or, alternatively, it must be expressed on the axon and/or growth cone itself. Second, the molecule must be expressed in a spatially restricted pattern consistent with the trajectory of the axon. Widely expressed guidance molecules would only provide conflicting cues for growth cones. Third, the molecule has to be presented in the correct temporal sequence. Guidance cues must be expressed when axons are actively navigating a pathway. Finally, the trajectory of axons must be perturbed when the function of the putative guidance molecule is disrupted. In the present study we have identified NOC-2, a novel cell-surface carbohydrate that meets all the criteria for a specific axon guidance molecule in the embryonic *Xenopus* forebrain. NOC-2 was identical to or closely related to human blood group A trisaccharide and was present on two glycoproteins of molecular mass 195 and 205 kDa in *Xenopus* brain. The 195 kDa glycoprotein is a novel glycoform of the neural cell adhesion molecule N-CAM, while the identity of the 205 kDa glycoprotein remains unclear. Whole-mount immunohistochemical staining of *Xenopus* embryonic brain revealed that NOC-2 was expressed by a discrete subpopulation of growing axons that form a stereotypical pathway. The trajectory of these axons was severely disrupted in the presence of either soluble blood group A trisaccharide or when NOC-2 was blocked with antibodies. Therefore, NOC-2 is a bona fide

axon guidance molecule active during formation of the early scaffold of axon tracts within the embryonic vertebrate brain.

Cell surface carbohydrates have previously been implicated, both directly and indirectly, in specific cellular interactions in the developing nervous system. For instance, the presence of polysialic acid side chains on N-CAM modulates the adhesiveness of cells by affecting both N-CAM- and L1-mediated binding (Hoffman and Edelman, 1983; Rutishauser and Landmesser, 1991). The long polysialic acid residues are highly negatively charged and appear to inhibit adhesion via both electrostatic repulsion and steric hindrance (Yang et al., 1992). Carbohydrates on L1 mediate cis-interactions with N-CAM and modulate neurite outgrowth (Kadmon et al., 1990a,b; Horstkorte et al., 1993; Heiland et al., 1998). The HNK-1 carbohydrate epitope present on N-CAM and L1 acts directly as a ligand in cell-mediated interactions (Kunemund et al., 1988; Hall et al., 1993, 1997). Cell-surface galactose moieties are involved in axon growth by acting as ligands for carbohydrate receptors such as cell surface glycosyltransferases (Shur, 1991, 1993). Substrate-immobilized sugars can also stimulate neurite outgrowth by some cells (Puche and Key, 1996; Puche et al., 1997). Thus, the differential expression of cell surface carbohydrates by subpopulations of neurons may be an important means for regulating the growth behaviour of axons in vivo.

How does NOC-2 mediate selective interactions between axons at the SOT-TPOC junction in embryonic *Xenopus* brain? One possibility is that NOC-2 on SOT axons is a ligand for carbohydrate-binding receptors present on the surface of axons in the ventral portion of the TPOC. Alternatively, the endfeet of neuroepithelial cells underlying the SOT-TPOC junction could either secrete soluble bivalent receptors which selectively fasciculate NOC-2^+ axons or they could express cell surface receptors themselves. Previous studies have demonstrated that soluble bivalent lectins such as galectin-1 are co-expressed with their ligands at sites of selective axon fasciculation in the spinal cord and olfactory bulb of rodents (Regan et al., 1986; Key and Akeson, 1993; Puche and Key, 1995, 1996). Zipser and colleagues revealed that subpopulations of sensory afferents expressing a 130 kDa mannose-containing glycoprotein project as a tightly fasciculated bundle within the periphery, but defasciculate upon entering the nerve cord in leech. Defasciculation was mediated by mannose-binding receptors present on the surface of neuroepithelial cells at the entry point of peripheral afferents into the nerve cord (Zipser et al., 1989; Zipser and Cole, 1991; Song and Zipser, 1995). Guidance cues are also believed to be present on neuroepithelial cells at the junction of the posterior commissure and TPOC in Zebrafish (Chitnis and Kuwada, 1991; Chitnis et al., 1992) and within the optic tract in *Xenopus* (Harris, 1989). Our results favour the presence of receptors for NOC-2 on the surface of axons in the ventral TPOC since axon guidance is perturbed when they are ablated. However, the expression of additional receptors on the endfeet of neuroepithelial cells underlying the SOT-TPOC junction could explain why we observed some SOT axons that followed a normal trajectory in the absence of a TPOC. There are probably guidance cues other than NOC-2 present at the SOT-TPOC junction since some NOC-2^+ axons are able to navigate through this choice point correctly even in the presence of exogenous BGA. This was not surprising since we showed that the NOC-2 population of axons is heterogenous with respect to expression of cell surface carbohydrates. Some of these axons co-expressed NOC-1 and there may be other, as yet, unidentified subpopulations that express different guidance cues.

NOC-2 appears to have specific roles at different points in the trajectory of axons expressing this molecule. In addition to its role in mediating turning at the SOT-TPOC junction, NOC-2 is also involved in the growth of axons across the rostral midline within the POC. Blocking of NOC-2 function led to axons straying from the presumptive telencephalic nucleus into inappropriate terrorities rather than forming fasciculated bundles that crossed the midline within the POC. Although NOC-2 appeared to be essential for axons to fasciculate within the POC, once these axons had entered the TPOC their growth was independent of NOC-2 and they continued to grow longitudinally until they reached the TPOC-ventral commissure junction. The turning of NOC-2^+ axons from the TPOC into the ventral commissure was mediated in part by NOC-2. When NOC-2 function was perturbed axons became disoriented and either stalled or grew dorsally instead of ventrally at the TPOC-ventral commissure junction. These results suggest that NOC-2 receptors are expressed by neuroepithelial cells underlying the pathway and that they provide cues to turn ventrally. The fact that some NOC-2^+ axons do not respond to these cues and instead continue to grow longitudinally into the ventral longitudinal tract indicates that this subpopulation of axons is functionally heterogenous at this choice point. Therefore NOC-2 may not be the only guidance cue associated with the turning of NOC-2^+ axons at the TPOC-ventral commissure junction. We have recently identified a role for chondroitin sulphate proteoglycans in axons turning at this junction (Anderson et al., 1998). These molecules could be redundant cues or they could be part of the receptor complex for NOC-2. Since chondroitin sulfate proteoglycans can modulate N-CAM mediated axon growth (Friedlander et al., 1994) they could be involved in regulating the function of the NOC-2 glycoform of N-CAM at the TPOC-ventral commissure junction.

N-CAM glycoform variants are not unique to *Xenopus*, as two further glycoforms, NOC-3 and NOC-4, were identified on primary olfactory axons in rat (Dowsing et al., 1997). This raises the possibility that other subpopulations of axons may also exist in *Xenopus*. In fact we showed that there were at least three chemically distinct subpopulations of axons in *Xenopus* embryonic brain. Axons expressed either NOC-1 alone, or NOC-2 alone, or both NOC-1 and NOC-2 together. The results of the present study have led us to a model for growth cone guidance in the embryonic vertebrate forebrain. We postulate the presence of multiple subpopulations of growing axons that express specific cell surface carbohydrates on their axons and growth cones. These carbohydrates are ligands for carbohydrate-binding receptors that mediate diverse cellular behaviours such as selective fasciculation of axons and contact-mediated turning of growth cones at axon tract junctions. These interactions enable a template of axon pathways to be established and provide the necessary guidance cues for subsequent axon tract formation.

This study was supported by an Australian NH&MRC grant to B. K. and by a University of Melbourne Faculty of Medicine scholarship to R. B. A.

REFERENCES

Akeson, R. A., Wujek, J. R., Roe, S., Warren, S. L. and Small, S. J. (1988). Smooth muscle cells transiently express NCAM. *Brain Res.* **464**, 107-120.
Anderson, R. B. and Key, B. (1996). Expression of a novel N-CAM

glycoform (NOC-1) on axon tracts in embryonic Xenopus brain. *Dev. Dyn.* **207**, 263-269.

Anderson, R. B., Walz, A., Holt, C. E. and Key, B. (1998). Chondroitin sulfates modulate axon guidance in embryonic Xenopus brain. *Dev. Biol.* **202**, 235-243.

Baier, H., Klostermann, S., Trowe, T., Karlstrom, R. O., Nusslein-Volhard, C. and Bonhoeffer, F. (1996). Genetic dissection of the retinotectal projection. *Development* **123**, 415-425.

Chien, C.-B., Rosenthal, D. E., Harris, W. A. and Holt, C. E. (1993). Navigational errors made by growth cones without filopodia in the embryonic *Xenopus* brain. *Neuron* **11**, 237-251.

Chitnis, A. B. and Kuwada, J. Y. (1991). Elimination of a brain tract increases errors in pathfinding by follower growth cones in the zebrafish embryo. *Neuron* **7**, 277-285.

Chitnis, A. B., Patel, C. K., Kim, S. and Kuwada, J. Y. (1992). A specific brain tract guides follower growth cones in two regions of the zebrafish brain. *J. Neurobiol.* **23**, 845-854.

Chu, D. T. W. and Klymkowsky, M. W. (1989). The appearance of acetylated α-tubulin during early development and cellular differentiation in *Xenopus*. *Dev. Biol.* **136**, 104-117.

Dodd, J. and Jessell, T. (1998). Axon guidance and the patterning of neuronal projections in vertebrates. *Science* **242**, 692-699.

Dowsing, B., Puche, A., Hearn, C. and Key, B. (1997). Presence of novel N-CAM glycoforms in the rat olfactory system. *J. Neurobiol.* **32**, 659-670.

Elkins, T., Hortsch, M., Bieber, A. J., Snow, P. M. and Goodman, C. S. (1990). Drosophila fasciclin I is a novel homophilic adhesion molecule that along with fasciclin III can mediate cell sorting. *J. Cell Biol.* **110**, 1825-1832.

Friedlander, D. R., Milev, P., Karthikeyan, L., Margolis, R. K., Margolis, R. U. and Grumet, M. (1994). The neuronal chondroitin sulfate proteoglycan neurocan binds to the neural cell adhesion molecules Ng-CAM/L1/NILE and N-CAM, and inhibits neuronal adhesion and neurite outgrowth. *J. Cell Biol.* **125**, 669-680.

Grenningloh, G., Bieber, A., Rehm, E. J., Snow, P. M., Traquina, Z., Hortsch, M., Patel, N. H. and Goodman, C. S. (1990). Molecular genetics of neuronal recognition in Drosophila: evolution and function of immunoglobulin superfamily cell adhesion molecules. *Cold Spring Harbor Symp. Quant. Biol.* **55**, 327-340.

Hall, H., Carbonetto, S. and Schachner, M. (1997). L1/HNK-1 carbohydrate- and beta 1 integrin-dependent neural cell adhesion to laminin-1. *J. Neurochem.* **68**, 544-553.

Hall, H., Liu, L., Schachner, M. and Schmitz, B. (1993). The L2/HNK-1 carbohydrate mediates adhesion of neural cell to laminin. *Euro. J. Neurosci.* **5**, 34-42.

Harrelson, A. L. and Goodman, C. S. (1988). Growth cone guidance in insects: fasciclin II is a member of the immunoglobulin superfamily. *Science* **242**, 700-708.

Harris, W. A. (1989). Local positional cues in the neuroepithelium guide retinal axons in embryonic Xenopus brain. *Nature* **339**, 218-221.

Hartenstein, V. (1993). Early pattern of neuronal differentiation in the *Xenopus* embryonic brainstem and spinal cord. *J. Comp. Neurol.* **328**, 213-231.

Heiland, P. C., Griffith, L. S., Lange, R., Schachner, M., Hertlein, B., Traub, O. and Schmitz, B. (1998). Tyrosine and serine phosphorylation of the neural cell adhesion molecule L1 is implicated in its oligomannosidic glycan dependent association with NCAM and neurite outgrowth. *Eur. J. Cell Biol.* **75**, 97-106.

Hoffman, S. and Edelman, G. M. (1983). Kinetics of homophilic binding by embryonic and adult forms of the neural cell adhesion molecule. *Proc. Natl. Acad. Sci. USA* **80**, 5762-5766.

Holtfreter, J. (1943). Properties and function of the surface coat in amphibian embryos. *J. Exp. Zool.* **93**, 251-323.

Horstkorte, R., Schachner, M., Magyar, J. P., Vorherr, T. and Schmitz, B. (1993). The fourth immunoglobulin-like domain of NCAM contains a carbohydrate recognition domain for oligomannosidic glycans implicated in association with L1 and neurite outgrowth. *J. Cell Biol.* **121**, 1409-1421.

Kadmon, G., Kowitz, A., Altevogt, P. and Schachner, M. (1990a). The neural cell adhesion molecule N-CAM enhances L1-dependent cell-cell interactions. *J. Cell Biol.* **110**, 193-208.

Kadmon, G., Kowitz, A., Altevogt, P. and Schachner, M. (1990b). Functional cooperation between the neural adhesion molecules L1 and N-CAM is carbohydrate dependent. *J. Cell Biol.* **110**, 209-218.

Karlstrom, R. O., Trowe, T., Klostermann, S., Baier, H., Brand, M., Crawford, A. D., Grunewald, B., Haffter, P., Hoffmann, H., Meyer, S. U., Muller, B. K., Richter, S., van Eeden, F. J., Nusslein-Volhard, C. and Bonhoeffer, F. (1996). Zebrafish mutations affecting retinotectal axon pathfinding. *Development* **123**, 427-438.

Key, B. and Akeson, R. A. (1990). Olfactory neurons express a unique glycosylated form of the neural cell adhesion molecule (N-CAM). *J. Cell Biol.* **110**, 1729-1743.

Key, B. and Akeson, R. A. (1991). Delineation of olfactory pathways in the frog nervous system by unique glycoconjugates and N-CAM glycoforms. *Neuron* **6**, 381-396.

Key, B. and Akeson, R. A. (1993). Distinct subsets of sensory olfactory neurons in mouse: possible role in the formation of the mosaic olfactory projection. *J. Comp. Neurol.* **335**, 355-368.

Kunemund, V., Jungalwala, F. B., Fischer, G. Chou, D. K. H., Keilhauer, G. and Schachner, M. (1988). The L2/HNK-1 carbohydrate of the neural cell adhesion molecules is involved in cell interactions. *J. Cell Biol.* **106**, 213-223.

Kuwada, J. Y. (1986). Cell recognition by neuronal growth cones in a simple vertebrate embryo. *Science* **233**, 740-746.

Lin, D. M., Fetter, R. D., Kopczynski, C., Grenningloh, G. and Goodman, C. S. (1994). Genetic analysis of Fasciclin II in Drosophila: defasciculation, refasciculation, and altered fasciculation. *Neuron* **13**, 1055-1069.

Macdonald, R., Scholes, J., Strahle, U., Brennan, C., Holder, N., Brand, M. and Wilson, S. W. (1997). The Pax protein Noi is required for commissural axon pathway formation in the rostral forebrain. *Development* **124**, 2397-2408.

Macdonald, R., Xu, Q., Barth, K. A., Mikkola, I., Holder, N., Fjose, A., Krauss, S. and Wilson, S. W. (1994). Regulatory gene expression boundaries demarcate sites of neuronal differentiation in the embryonic zebrafish forebrain. *Neuron* **13**, 1039-1053.

Nelson, R. M., Venot, A., Bevilacqua, M. P., Linhardt, R. J. and Stamenkovic, I. (1995). Carbohydrate-protein interactions in vascular biology. *Annu. Rev. Cell Dev. Biol.* **11**, 601-631.

Nieuwkoop, P. D. and Faber J. (1956). *Normal Table of* Xenopus laevis (Daudin), pp. 162-188. North Holland Publishing Company, Amsterdam.

Puche, A. C., Bartlett, P. F. and Key, B. (1997). Substrate-bound carbohydrates stimulate signal transduction and neurite outgrowth in an olfactory neuron cell line. *Neuroreport* **8**, 3183-3188.

Puche, A. C. and Key, B. (1995). Identification of cells expressing galectin-1, a galactose-binding receptor, in the rat olfactory system. *J. Comp. Neurol.* **357**, 513-523.

Puche, A. C. and Key, B. (1996). N-acetyl-lactosamine in the rat olfactory system: Expression and potential role in neurite growth. *J. Comp. Neurol.* **364**, 267-278.

Raper, J. A., Bastiani, M. and Goodman, C. S. (1983). Pathfinding by neuronal growth cones in grasshopper embryos. *J. Neurosci.* **3**, 31-41.

Regan, L. J., Dodd, J., Barondes, S. H. and Jessell, T. M. (1986). Selective expression of endogenous lactose-binding lectins and lactoseries glycoconjugates in subsets of rat sensory neurons. *Proc. Natl. Acad. Sci. USA* **83**, 2248-2252.

Ross, L. S., Parrett, T. and Easter, S. S. (1992). Axonogenesis and morphogenesis in the embryonic zebrafish brain. *J. Neurosci.* **12**, 467-482.

Rutishauser, U. and Landmesser, L. (1991). Polysialic acid on the surface of axons regulates patterns of normal and activity-dependent innervation. *Trends Neurosci.* **14**, 528-532.

Shur, B. D. (1991). Cell surface 1,4 galactosyltransferase: twenty years later. *Glycobiol.* **1**, 563-575.

Shur, B. D. (1993). Glycosyltransferases as cell adhesion molecules. *Curr. Opin. Cell Biol.* **5**, 854-863.

Snow, P. M., Zinn, K., Harrelson, A. L., McAllister, L., Schilling, J., Bastiani, M. J., Makk, G. and Goodman, C. S. (1988). Characterisation and cloning of Fasciclin I and II glycoproteins in the grasshopper. *Proc. Natl. Acad. Sci. USA* **85**, 5291-5295.

Song, J. and Zipser, B. (1995). Targeting of neuronal subsets mediated by their sequentially expressed carbohydrate markers. *Neuron* **14**, 537-547.

Wilson, S. W. and Easter, S. S. (1991). Stereotyped pathway selection by growth cones of early epiphysial neurons in the embryonic zebrafish. *Development* **112**, 723-746.

Wilson, S. W., Placzek, M. and Furley, A. J. (1993). Border disputes: do boundaries play a role in growth-cone guidance? *Trends Neurosci.* **16**, 316-323.

Yang, P., Yin, X. and Rutishauser, U. (1992). Intercellular space is affected by the polysialic acid content of NCAM. *J. Cell Biol.* **116**, 1487-1496.

Zipser, B. and Cole, R. N. (1991). A mannose-specific recognition mediates the defasciculation of axons in the leech CNS. *J. Neurosci.* **11**, 3471-3480.

Zipser, B., Morell, R. and Bajt, M. L. (1989). Defasciculation as a neuronal pathfinding strategy: involvement of a specific glycoprotein. *Neuron* **3**, 621-630.